Metabolic and Growth Rate Alterations in Lymphoblastic Cell Lines Discriminate Between Down Syndrome and Alzheimer Disease

Pinar Coskun[1*], Pablo Helguera[1,2], Zahra Nemati[1], Ryan C. Bohannan[1], Jean Thomas[1], Samuel E. Schriner[3], Jocelyn Argueta[1], Eric Doran[4], Douglas C. Wallace[5], Ira T. Lott[4], Jorge Busciglio[1*]

[1]Department of Neurobiology and Behavior, Institute for Memory Impairments and Neurological Disorders (iMIND), and Center for the Neurobiology of Learning and Memory (CNLM), University of California, Irvine, CA.

[2]Instituto de Investigación Médica Mercedes y Martin Ferreyra, Córdoba, Argentina

[3]Department of Pharmaceutical Science, University of California, Irvine, CA.

[4]Department of Pediatrics, University of California, Irvine, CA.

[5]Center for Mitochondrial and Epigenomic Medicine (CMEM), Children's Hospital of Philadelphia, and Department of Pathology and Laboratory Medicine, University of Pennsylvania, Philadelphia, PA.

Corresponding authors:

Pinar Coskun, M.D.

Department of Neurobiology and Behavior,
Institute for Memory Impairments and Neurological Disorders (iMIND),
University of California, Irvine
3400C Biological Sciences III, Irvine, CA 92617
Phone: (949) 350 7007 Fax: (949) 824 2447
pinar@uci.edu

Jorge Busciglio, Ph.D.

Department of Neurobiology and Behavior,
Institute for Memory Impairments and Neurological Disorders (iMIND),
University of California, Irvine
3216 Biological Sciences III, Irvine, CA 92617
Phone: (949) 824-4820 Fax: (949) 824 2447

jbuscigl@uci.edu

Key Words:

Down syndrome

Dementia

Alzheimer Diseases

Mitochondrial Dysfunction

Oxidative stress

Metabolic alterations

Lymphoblastoid cell lines

Autophagy

Growth retardation

Abstract

Background: Deficits in mitochondrial function and oxidative stress play pivotal roles in Down syndrome (DS) and Alzheimer's disease (AD) and these alterations in mitochondria occur systemically in both conditions.

Objective: We hypothesized that peripheral cells of elder subjects with DS exhibit disease-specific and dementia-specific metabolic features. To test this, we performed a comprehensive analysis of energy metabolism in lymphoblastic-cell-lines (LCLs) derived from subjects belonging to four groups: DS-with-dementia (DSAD), DS-without-dementia (DS), sporadic AD and age-matched controls.

Methods: LCLs were studied under regular or minimal feeding regimes with galactose or glucose as primary carbohydrate sources. We assessed metabolism under glycolysis or oxidative phosphorylation by quantifying cell viability, oxidative stress, ATP levels, mitochondrial membrane potential (MMP), mitochondrial calcium uptake, and autophagy.

Results: DS and DSAD LCLs showed slower growth rates under minimal feeding. DS LCLs mainly dependent on mitochondrial respiration exhibited significantly slower growth and higher levels of oxidative stress compared to other groups. While ATP levels (under mitochondrial inhitors) and mitochondrial calcium uptake were significantly reduced in DSAD and AD cells, MMP was decreased in DS, DSAD and AD LCLs. Finally, DS LCLs showed markedly reduced levels of the autophagy marker LC3-II, underscoring the close association between metabolic dysfunction and impaired autophagy in DS.

Conclusion: There are significant mitochondrial functional changes in LCLs derived from DS, DSAD and AD patients. Several parameters analyzed were consistently different between DS, DSAD, and AD lines suggesting that metabolic indicators between LCL groups may be utilized as biomarkers of disease progression and/or treatment outcomes.

Introduction

A key feature of Down syndrome (DS) is the high predisposition of individuals to develop Alzheimer's disease (AD) [1-5]. Chronic oxidative stress and mitochondrial dysfunction are key factors, that are thought to contribute not only to the development of AD, but also to additional clinical conditions commonly observed in individuals with DS such as diabetes, immune system abnormalities and autism spectrum disorder [6-9]. Oxidative stress and metabolic deficiencies have been consistently observed in different DS primary cells including fibroblasts [10, 11], cortical neurons, astrocytes and pancreatic β cells [12]. These alterations are related to the presence of increased basal levels of mitochondrial reactive oxygen species (ROS), deficits in electron transport chain (ETC) components, and an adaptive down-regulation of mitochondrial activity. [12, 13]. Most of the studies reporting oxidative stress and metabolic defects in DS have been obtained examining fetal or young DS cells and tissues. However, little information is available with respect to metabolic changes in cells from mature and aged individuals with DS.

Given that a high number of individuals with DS develop AD dementia and virtually all of them develop AD neuropathology [3, 14], it would be critical to understand the changes in cellular metabolism associated with this transition as well as characterizing clinical biomarkers for disease progression. Based on findings from the literature and our own studies [15-22], we hypothesized that peripheral tissues from DS individuals may present disease state-related signature changes, with a particular emphasis on mitochondrial and metabolic parameters. From our previous study, we learnt that in DS with Alzheimer disease (DSAD) and AD brains and LCLs there is significantly more mtDNA mutations than in DS brains and LCLs [19]. Furthermore, mitochondrial dysfunction seems to play a critical role leading to intracellular deposition of $A\beta_{42}$, reduced levels of AβPPs, and a chronic state of increased neuronal vulnerability [10]. In this study, we tested for differential metabolic features in DS DS, DSAD, AD and control LCLs. Specifically, we assessed the growth profile and metabolic parameters of lymphoblastic cell lines (LCLs) generated from demented and non-demented individuals with DS, and compared them to those of sporadic AD and control LCLs. We found that DS, DSAD and AD exhibit different degree of mitochondrial defects and oxidative stress compared to controls. There was a clear growth retardation under minimal feeding conditions in DS and DSAD LCLs compared to AD and control cell lines. Furthermore, under oxidative conditions,

significant differences in metabolic function were apparent between DS and DSAD LCLs. Thus, LCLs reveal metabolic changes associated with the neurodegenerative process and point to cellular metabolic parameters as potential useful peripheral biomarkers of disease progression.

Materials And Methods

The study protocol was approved by the University of California, Irvine Institutional Review Board (IRB). Written informed consent was obtained from all cell donors.

Sample Collection and generation of LCLs: An EBV immortalization protocol was used to establish LCLs [23]. DS and DSAD blood samples were obtained during patient examinations of our current longitudinal cohort studies and were derived from subjects with confirmed full trisomy 21 subjects. Eight to twelve LCLs were analyzed in each group (control, DS, DSAD and sporadic AD). All subjects were in the age range of 40 to 70 years. Detailed demographic information is listed in table 1. Three to six subjects of each gender were tested for each assay. Results are reported as a combination of male and female LCLs for each group. Venous blood samples were collected in 10 mL yellow-top tubes containing acid citrate/dextrose solution. After 3 days at room temperature, the plasma fraction was removed by centrifugation at 800 rpm for 15 min. The red blood cell and buffy coat fractions were diluted 1:1 in RPMI 1640 (Life Technologies), layered on pre-prepared Histopaque 1077 (Sigma-Aldrich) gradients and centrifuged at 1100 rpm for 45 min. The white fraction above the fluffy layer containing lymphocyte cells was collected for EBV transformation. Previously prepared virus cocktails from Epstein-Barr virus-infected marmoset cells, line B95-8 was used for transformation under cyclosporine treatment [23]. After 2 to 3 weeks of expansion, established cell lines were stored in liquid nitrogen.

LCL culture conditions: Cells were maintained in RPMI 1640 medium without glucose (Life Sciences) supplemented with 15% FBS and 2mM L-Glutamine. In order to assess glycolytic metabolism, cells were kept in 2 gr/L glucose with regular FBS. To assess oxidative metabolism, cells were switched and adapted to medium containing 2 gr/L galactose instead of glucose and 15% dialyzed FBS. After thawing, cells were grown for 5 days before experimentation.

Karyotyping: LCLs were incubated in 5 μg/mL colchicine (Sigma-Aldrich) for 3 hr. Colchicine was added 1 hr after a medium change. Cells were centrifuged at 1000 rpm for 5 min and resuspended in hypotonic KCl (0.56%) at 37^{o}C for 20 min. Then the cells were gently fixed with methanol:acetic acid (3:1) at 4^{o}C for 30 min. Chromosome spreading was performed as described [24] and analyzed under a fluorescent microscope. Images were taken at 100X magnification and processed with Image J software for chromosome counting.

Mitochondrial membrane potential and mtPTP activation: Cells at 5x10^{8} total density were permeabilized in 0.02% digitonin (Sigma-Aldrich) for 5 minutes and incubated on ice in H-buffer (225mM mannitol, 75mM sucrose, 10mM MOPS, 1mM EGTA and 0.5% fat free BSA at pH 7.2). Cells were pelleted by centrifugation at 1000 rpm for 5 min and resuspended in reaction buffer (250 mM sucrose, 10 mM MOPS, 2 mM K_2HPO_4, 5 mM succinate, pH 7.2). Mitochondrial fractions were resuspended in 4 μl aliquots, centrifuged 2 min at 10,000 g and brought to 200 μl in isolation buffer without BSA. Protein level was quantified using the Bradford method. Mitochondrial membrane potential and permeability transition (mtPTP) were measured using the fluorescent probe rhodamine 123 (Molecular Probes, Life Technology) using a Perkin Elmer LS50B luminescent spectrophotometer set at excitation/emission 490/535 nm. One mg of mitochondrial protein was added to 3 ml of reaction buffer at 30°C. Fluorescence was allowed to stabilize and then $CaCl_2$ was added in sequential aliquots of 15 or 25 nmol, each associated with a transient increase in fluorescence. Activation of the mtPTP and collapse of the electrochemical gradient was signaled by the maximum rise and stabilization of fluorescence.

Rhodamine 123 concentrations were quantified using a standard curve, and membrane potential was calculated using the Nernst equation [25]. The concentration was calculated using the minimum level of fluorescence after the addition of mitochondria ($F_{outside}$) and the internal concentration measured as the difference between the total concentration (maximum fluorescence obtained after $CaCl_2$ addition, F_{total}) and the concentration outside (F_{total} - $F_{outside}$ = $F_{internal}$). Mitochondrial volume was set at 1 μl /μg as previously described [26].

Growth/proliferation assays: Growth curves were measured at multiple times containing all four groups with 4 to 6 LCLs in each group and each sex. The growth experiment was designed to analyze glycolytic and oxidative behavior of LCLs under regular and minimal feeding conditions. Each LCL was set up at 3x10^{5} cells/mL, 10 ml plating volume for both glucose and galactose based media. Cell counts were performed using a hemocytometer and

collected every other day up to day 15. Regular feeding regime was applied every other day to keep cell density below 10^6 cell/mL. Minimal feeding conditions were maintained throughout the experiments at 10 ml total volume by adding 1 to 2 ml of RPMI 1640 with 2mM L-glutamine every 4 days.

ROS quantification: Mitochondrial H_2O_2 levels were measured using the fluorescent probe MitoSOX (Molecular Probes, Life Technology). Cells primed in glucose and galactose conditions were incubated in 5 μM MitoSOX 30 min at 37°C in HANK'S balanced salt solution. After two washes, the cells were plated at 100,000 cell/well in 96-well plates in triplicate wells. Fluorescence was measured at excitation/emission 510/580 nm in a fluorescent reader (Molecular Devices Gemini EM). Total cellular ROS levels were measured using the fluorescent probe CM-H_2DCFDA (Molecular Probes, Life Technologies). In addition to baseline measures, paraquat (*N*,*N*′-dimethyl-4,4′-bipyridinium dichloride) (pQ) was used to induce oxidative stress. pQ converts molecular oxygen to superoxide anion and other ROS after reduction by cellular cytochrome P-450s and mitochondrial complex 1 (NADH dehydrogenase)[27]. LCLs plated at 100,000 cells/well in triplicate wells for each cell line were treated with 250 μM pQ or vehicle for 48 hr. Then, the cells were incubated in 5 μM CM-H_2DCFDA for 30 min, washed twice, and the fluorescence was measured at excitation/emission of 495/525nm.

ATP measurements: 100,000 cells/well were plated on pre-coated poly-lysine (Sigma-Aldrich) white opaque 96 well plates. Total ATP levels were measured using a commercial kit (Perkin-Elmer ATP-Lite) at baseline and after 30 min of incubation with 100 μM FCCP and 10 μM rotenone, 3.6 μM antimycin, and 5 μM oligomycin. Luminescence was measured using a Beckman LD-400 luminometer. Each cell line was assayed in triplicate wells. Values were normalized using total cell number/well.

Western Blot: Cells were collected and cell pellets were frozen at -80° C. Then the samples were rapidly thawed and resuspended in RIPA buffer (10% deoxycholic acid, 1M Tris HCl pH:7.5, 5M NaCl, 10% Triton X, 10% SDS) plus protease and phosphatase inhibitors (Roche). Equal amounts of protein (20ug/sample) were separated on 4-12% Bis-Tris gels (BioRAD), transferred to nitrocellulose membranes and blocked for 1 hr (StartingBlock, Thermo Scientific). Membranes were incubated overnight at 4°C with anti-LC3 (1:1000, Cell Signaling) and anti-GAPDH (1:5000, Abcam) antibodies. Then, the membranes were washed with 0.1% Tween 20/Tris-buffer (pH 7.5) and incubated with horseradish peroxidase-conjugated secondary

antibodies (1:10,000, Pierce Biotechnology) for 1 hr. Blots were developed using a chemiluminescence kit (Super Signal, Thermo Scientific) and quantified using Image J.

Results

Full chromosome 21 trisomy was confirmed in all DS and DSAD cell lines. All control and ADs LCLs were euploid. Thus, the immortalization process did not affect the primary cells' original karyotypes.

Reduced mitochondrial membrane potential in DS, DSAD and ADs LCLs.

Mitochondrial membrane potential (MMP) was analyzed using the fluorescent probe rhodamine 123. MMP is a critical functional parameter of electron transport chain function, which generates and maintains the MMP. We obtained MMP values of 180.2 mV in controls, 170.1 mV in DS, 167.8 mV in DSAD and 159.8 mV in AD LCLs (Figure 1A). Thus, we found significant reductions in MMP in DS, DSAD and AD compared to control LCLs (*p=0.03, ANOVA),* indicating alterations in mitochondrial function in LCLs derived from all three disease groups.

Differential mitochondrial calcium uptake discriminates between DS, DSAD and AD LCLs.

Mitochondria play a major role maintaining low cellular calcium levels by taking up calcium when cytosolic levels increase. Elevated cytosolic [Ca^{++}] levels leads to the collapse of the MMP and induces the formation of the mitochondrial permeability transition pore (mPTP) leading to apoptosis. Hence, mitochondrial calcium uptake capacity represents a threshold for the initiation of programmed cell death [28]. We measured mitochondrial calcium uptake before mPTP formation in LCLs. Control LCLs required 109.0 nmoles of calcium to initiate mPTP opening, while DS, DSAD and AD LCLs required 96.8, 67.8 and 67.2 nmoles, respectively (*ANOVA p<0.05*)(Figure 1B). DSAD and AD LCLs exhibited significantly low calcium uptake capacity suggesting that changes in the ability of mitochondria to modulate intracellular [Ca^{++}] levels and hence increased susceptibility to apoptotic stimuli are associated with AD in patient-derived LCLs.

DS and DSAD LCLs exhibit impaired proliferative capacity.

LCLs utilize glycolysis to generate ATP in glucose-containing medium. However, replacing glucose with galactose forces LCLs to switch to oxidative phosphorylation for ATP production [29] We evaluated the proliferation of LCLs in glucose- or galactose-containing medium under minimal feeding conditions, a useful paradigm to study metabolic defects, autophagy and differential stress-induced responses in gene expression in several disease paradigms [30, 31]. All LCLs groups exhibited similar growth rates in regular culture medium and normal feeding conditions (Figure S1). Consistent with previous reports, LCLs proliferation was slower in galactose- than in glucose-based medium (Figure 2 and Figure S1)[32].

Under minimal feeding regime, DS and DSAD LCLs grew significantly slower in both glucose- and galactose-based media (Figure 2). In glucose medium, marked differences were apparent during the first week (Figure 2A). Both DS and DSAD LCLs reached the growth plateau by 10 days, while CTR LCLs typically grew steadily until day 13 *(p=0.001 ANOVA*). In contrast, AD LCLs proliferated even faster than CTR LCLs but, similar to DS and DSAD LCLs, reached a growth plateau at day 10. As a result of the slower growth rate, DS and DSAD LCLs reached the growth plateau at approximately 50% lower cellular density (i.e., ~$6x10^6$ total cells/well) than control and AD LCLs (i.e. ~$12x\ 10^7$ total cells/well) (Figure 2A). It has been reported that AD LCLs grow faster under normal glycolytic condition than CTR LCLs [33]. Interestingly we didn't observe a similar phenomenon under normal feeding condition but a similar tren was indeed observed under minimal feeding conditions even though the difference in growth rate between AD and CTR LCLs did not reach statistical significance.

In galactose-containing medium, control and AD LCLs proliferated steadily reaching the growth plateau around day 12/13 (Figure 2B). Under galactose, the total number of cells was approximately an order of magnitude lower than in glucose-containing medium. DS LCLs exhibited modest growth reaching the plateau by day 3. Interestingly, minimal feeding conditions in galactose-based medium revealed a significant difference in growth rates between DS and DSAD LCLs (Figure 2B, compare green [DS] and red [DSAD] curves). AD LCLs grew steadily and similar to control LCLs during the first 7 days, exhibiting a major difference in cell number compared to DSAD (*p=0.03*). Thus, growth rates in glucose- and galactose-containing medium

and minimal nutrient availability expose significant differences in growth rates between DS, DSAD and AD LCLs.

Differential response patterns of DS, DSAD and ADs LCLs to oxidative stress.

In most cells, mitochondria normally produce ROS as a byproduct during ATP generation that are neutralized by specific antioxidant mechanisms [34]. However, under stressful or toxic states, ROS levels can overwhelm the antioxidant defense mechanisms and produce structural cellular damage [34, 35]. Since DS, DSAD and AD LCLs exhibit significantly low MMP, a strong indication of mitochondrial dysfunction, we analyzed ROS levels. We measured baseline cellular ROS levels and the resilience of LCLs to toxins that increase free radical production such as pQ. We measured cellular ROS using the fluorescent probe DCF. Under basal conditions DS LCLs displayed significantly higher ROS levels compared to the other 3 groups *(ANOVA $p=0.04$)*(Figure 3A). PQ treatment increased ROS levels in all groups *(two way ANOVA $p<0.05$)*, but DSAD LCLs showed the largest increase with pQ treatment (*$p=0.006$*).
Next we studied mitochondrial ROS (mROS) production in both glucose and galactose media. In galactose medium, DS, DSAD and AD LCLs showed increased levels of mROS (DS and AD) (Figure 3B). The increase in mROS in DS LCLs was more prominent than in the other groups.
In glucose, DS, DSAD and AD LCLs exhibited a consistent 75% decrease in ROS production compared to control LCLs *($p<0.008$).* Taken together these results suggest that DS, DSAD and AD LCLs resort to glycolysis to avoid excess mROS production during oxidative phosphorylation.

We also assessed the effect of mitochondrial inhibitors on ATP levels. Quantifications were performed at baseline and after 30 min of combined treatment with the electron transport/ATP synthesis inhibitors rotenone, antimycin and oligomycin (i.e. RAO) [36]. There was no difference in ATP production between LCL groups at baseline (Figure 3C). However, treatment with RAO induced a significant reduction in ATP production in DSAD and AD LCLs (Figure 3C) indicating increased susceptibility of DSAD and AD LCLs to mitochondrial insults.

Differential LC3-II expression levels in DS, DSAD and AD LCLs.

Limitation of carbon sources is the most extensively studied condition that induces autophagy. Reduced autophagy has been reported in frontal cortex of elderly DS and AD patients [37]. Since mitochondrial dysfunction and increased ROS are proposed to initiate autophagy under nutrition-deprived conditions [38], we investigated whether DS growth retardation could be associated with abnormal, systemic autophagy in DS and AD. We evaluated autophagy on LCLs using the marker microtubule-associated protein 1 (LC3). LC3 is converted from a cytosolic form (LC3-I) to a lipidated form (LC3-II) upon autophagy induction, and it is then inserted into autophagosome membranes. Therefore, increased cellular levels of LC3-II are a direct indicator of autophagy activation [39-41]. We observed reduction of LC3-II levels in glucose-primed DS, DSAD and ADs LCLs (Figure 4A)*($p<0.003$, $p<0.03$, $p=0.06$ respectively ANOVA*) in agreement with a previous report in brain tissue [37]. Surprisingly, LC3-II levels were significantly lower in all four groups of LCLs primed with galactose compared to the same groups maintained in glucose-containing medium (Figure 4A and B, *two way ANOVA $p<0.001$*). However, only DS LCLs showed a significant reduction of LC3-II under galactose primed medium (Figure 4B)*($p<0.003$, ANOVA)*. DS LCLs showed a marked reduction in LC3-II levels in both glucose- and galactose-containing medium, indicating that autophagy is impaired in DS LCLs compared to DSAD and AD LCLs, possibly as a consequence of chronically increased baseline cellular ROS [41].

Discussion

Available evidence indicates the existence of increased oxidative stress and mitochondrial dysfunction in peripheral cells such as fibroblasts, amniocytes and LCLs in subjects with DS [11, 17, 42, 43]. LCLs derived from young individuals with DS (3 to 14 years of age) exhibited reduced oxygen consumption suggesting compromised mitochondrial bioenergetics [44]. The presence of mitochondrial defects in DS cells and tissues predicts alterations in cellular growth, which have been found in both mouse models of DS [45-47] and DS tissues [12, 48]. In this study, we performed direct comparisons of metabolic function and growth rates in LCLs generated from B-lymphocytes of patients with DS, DSAD, sporadic AD and age-matched control subjects. This is the first study to explore metabolic function in peripheral tissues across these disease groups.

We focused on parameters of mitochondrial function which, as shown previously, are consistently altered in DS primary cells derived from fetal tissues [12]. We not only found that mitochondrial alterations are present in LCLs from older patients with DS, but also that several of these parameters are differentially affected in DS, DSAD and AD LCLs (Table 2). For example, while MMP was significantly reduced across all three disease groups, the capacity to buffer [Ca^{++}] levels and maintain the electrochemical gradient was similar in control and DS LCLs but markedly lower in DSAD and AD LCLs. (Figure 1). These differences in MMP and calcium uptake could be related to different baseline mitochondrial [Ca^{++}] levels between the LCL groups. For example, AD transgenic mice exhibit low MMP and low mitochondrial calcium buffering capacity [49]. Thus, in our experiments, AD and DSAD baseline mitochondrial [Ca^{++}] levels may be higher than that of DS and CTR LCLs, therefore reducing the threshold to induce transition pore opening. The observed differential ROS levels in DS and DSAD, i.e. higher baseline ROS in DS than in the other groups can eventually lead to increased baseline mitochondrial calcium levels [50-55].

Several proteins encoded by chromosome 21 genes can modulate calcium signaling, including RCAN1 and DYRK1A [56, 57]. In DS and AD, calcium dishomeostasis could have a genetic or epigenetic origin since the expression of these same genes appears to be involved in regulating methylation [58, 59]. Ultimately, impaired modulation of calcium signaling leads to increased susceptibility to apoptotic stimuli associated with the presence of AD pathological changes, not only in the CNS but also in peripheral tissues and cells [60].

With respect to the higher baseline of ROS observed in DS cells, a recent study showed reduced H2O2 release to the extracellular medium by DS LCLs [61]. However, H2O2 release is the joint result of ROS production, metabolism, and degradation which involve multiple cellular pathways. This is substantially different than the direct measurements of cellular ROS levels applied in our study. Thus, additional experiments will be required to fully characterize ROS metabolism and catabolism in DS cells.

Differential results were also obtained after assessment of cellular proliferation. Proliferation of DS LCLs under regular feeding conditions was similar to normal LCLs, consistent with previous experiments utilizing skin fibroblasts [62]. However, when we limited the carbon source under oxidative phosphorylation or glycolysis, we found marked alterations: DS and DSAD LCLs under minimal glucose showed impaired growth. In galactose, which drives the cellular ATP supply from oxidative phosphorylation (i.e., mitochondrial-dependent state), there was a substantial difference in the growth rate of DS and DSAD LCLs, and both were clearly different from AD and control LCLs (Figure 2). We also examined the response of LCLs to oxidative stress, a prominent feature of DS pathology and a critical player during the aging process and in AD [63-65]. Under basal conditions, DS LCLs showed higher cellular ROS than the other groups. After induction of oxidative stress by pQ, both DS and DSAD exhibited larger increases in ROS levels than control and AD LCLs, likely due to the diminished capacity of aneuploid cells to withstand oxidative insults [66]. Interestingly, pQ treatment resulted in a significant induction of ROS specifically in DSAD cells indicating further impairment in antioxidant capacity related to the progression of AD. In this regard, it will be important to further examine the potential impact of amyloid-ß levels in peripheral tissues on cellular metabolism and free radical generation. When we examined mitochondrial ROS production in galactose-containing medium, we found increased ROS levels in DS, DSAD and AD LCLs, implying that both the genomic imbalance of trisomy 21 and AD-related changes contribute to mitochondrial oxidative stress. This interpretation is consistent with previous results indicating that, while AβPP overexpression is a critical factor driving AD pathology, imbalanced expression of other gene(s) located in chromosome 21 contribute significantly to the neurodegenerative process [67, 68]. ROS management becomes even more critical in the nervous system, where the vast majority of the cellular population is comprised of non-dividing cells.

Interestingly, AD LCLs exhibited a faster growth trend than the other LCLs groups under minimal feeding conditions. A similar result has been reported by de las Cuevas et al. [33]. The authors of that study proposed that AD LCLs have lower levels of p27 leading to enhanced cell division. In this regard, the slow growth of DS lines may be related to misregulation of p27 by chromosome 21 genes. For instance, DYRK1A phosphorylates p27 which in turn increases p27 degradation and reduced proliferation [69]. Thus, fluctuations in DYRK1A expression and

activity may underlie the differential growth between DS and DSAD LCLs. Future studies will focus on the modulation of the growth rate of DS and DSAD LCLs by DRYK1A.

Finally, we investigated the effect of limited nutrients on autophagy by analyzing levels of LC3-II, a structural component of autophagosomes [39, 40]. Autophagy serves to clear up and recycle damaged cellular structures, and to feed energy-dependent processes by catabolizing cellular energy molecules under nutritional deprivation [38, 70]. Importantly, oxidative stress has been proposed to be a converging point of autophagy induction for both states [71]. In our study, reduced LC3-II levels of glucose-primed DS, DSAD and AD LCLs compared to controls suggest that previously observed autophagy defects in DS and AD brains are not limited only to CNS cells but it is a systemic phenomenon [37]. It is plausible that reduced mitochondrial ROS and not total cellular ROS, is responsible for decreased autophagy in all three disease groups. A general reduction of LC3-II levels in galactose- compared to glucose-primed LCLs in all 4 groups would explain the slow growth rates under galactose conditions as observed by us and others [32]. However, significant reductions of LC3-II in DS LCLs compared to the other groups suggests impaired autophagy specific to DS. In fact, this would explain DS LCLs quiescent state and limited proliferation under galactose. Impaired autopaghy in galactose-primed DS LCLs may originate in chronic elevation of cellular ROS, oxidation of autophagy-related proteins and impaired LC3-II formation. These results indicate that, decreased autophagy is a prominent feature of DS LCLs directly linked to proliferation defects in DS LCLs.

In summary, the analysis of mitochondrial function and growth rates in LCLs generated from B-lymphocytes of DS, DSAD and AD subjects revealed a set of differentially altered metabolic parameters (Table 2). While the precise molecular mechanisms of these abnormalities is the focus of ongoing investigation, the results so far suggest that: 1. LCLs retain and express metabolic changes consistent with disease-specific states in DS and AD; 2. an array of these parameters may be suitable for development as indicators of disease state and progression; and 3. the presence of disease-specific alterations in proliferating cell lines derived from primary lymphocytes suggest that lymphocyte-derived iPSCs may also conserve critical pathological features to model disease mechanisms and investigate therapeutic options.

Acknowledgments

The Epstein-Barr virus-infected marmoset cell line B95-8 was kindly provided by Dr. Moyra Smith of UCI. This work was supported by NIH Alzheimer's Disease Research Center Grant AG16573, sub-project awards to I.T.L. D.C.W. and J.B, and a ADRC-UCI pilot project awarded to PEC. This project was also supported by the National Center for Research Resources and the National Center for Advancing Translational Sciences, NIH, through Grant UL1 TR000153. The study has no potential conflicts.

References

[1] Lai F, Williams RS (1989) A prospective study of Alzheimer disease in Down syndrome. *Arch Neurol* **46**, 849-853.

[2] Lemere CA, Blusztajn JK, Yamaguchi H, Wisniewski T, Saido TC, Selkoe DJ (1996) Sequence of deposition of heterogeneous amyloid beta-peptides and APO E in Down syndrome: implications for initial events in amyloid plaque formation. *Neurobiol Dis* **3**, 16-32.

[3] Lott IT, Head E (2005) Alzheimer disease and Down syndrome: factors in pathogenesis. *Neurobiol Aging* **26**, 383-389.

[4] Nistor M, Don M, Parekh M, Sarsoza F, Goodus M, Lopez GE, Kawas C, Leverenz J, Doran E, Lott IT, Hill M, Head E (2007) Alpha- and beta-secretase activity as a function of age and beta-amyloid in Down syndrome and normal brain. *Neurobiol Aging* **28**, 1493-1506.

[5] Weksler ME, Szabo P, Relkin NR, Reidenberg MM, Weksler BB, Coppus AM (2013) Alzheimer's disease and Down's syndrome: treating two paths to dementia. *Autoimmun Rev* **12**, 670-673.

[6] Dickinson MJ, Singh I (1993) Down's syndrome, dementia, and superoxide dismutase. *Br J Psychiatry* **162**, 811-817.

[7] Jovanovic SV, Clements D, MacLeod K (1998) Biomarkers of oxidative stress are significantly elevated in Down syndrome. *Free Radic Biol Med* **25**, 1044-1048.

[8] de Haan JB, Susil B, Pritchard M, Kola I (2003) An altered antioxidant balance occurs in Down syndrome fetal organs: implications for the "gene dosage effect" hypothesis. *J Neural Transm Suppl*, 67-83.

[9] Strydom A, Dickinson MJ, Shende S, Pratico D, Walker Z (2009) Oxidative stress and cognitive ability in adults with Down syndrome. *Prog Neuropsychopharmacol Biol Psychiatry* **33**, 76-80.

[10] Busciglio J, Pelsman A, Wong C, Pigino G, Yuan M, Mori H, Yankner BA (2002) Altered metabolism of the amyloid beta precursor protein is associated with mitochondrial dysfunction in Down's syndrome. *Neuron* **33**, 677-688.

[11] Valenti D, Manente GA, Moro L, Marra E, Vacca RA (2011) Deficit of complex I activity in human skin fibroblasts with chromosome 21 trisomy and overproduction of reactive oxygen species by mitochondria: involvement of the cAMP/PKA signalling pathway. *Biochem J* **435**, 679-688.

[12] Helguera P, Seiglie J, Rodriguez J, Hanna M, Helguera G, Busciglio J (2013) Adaptive downregulation of mitochondrial function in down syndrome. *Cell Metab* **17**, 132-140.

[13] Coskun P, Wyrembak J, Schriner SE, Chen HW, Marciniack C, Laferla F, Wallace DC (2012) A mitochondrial etiology of Alzheimer and Parkinson disease. *Biochim Biophys Acta* **1820**, 553-564.

[14] Head E, Lott IT (2004) Down syndrome and beta-amyloid deposition. *Curr Opin Neurol* **17**, 95-100.

[15] Nagy Z, Esiri MM, LeGris M, Matthews PM (1999) Mitochondrial enzyme expression in the hippocampus in relation to Alzheimer-type pathology. *Acta Neuropathol* **97**, 346-354.

[16] Kim SH, Fountoulakis M, Cairns N, Lubec G (2001) Protein levels of human peroxiredoxin subtypes in brains of patients with Alzheimer's disease and Down syndrome. *J Neural Transm Suppl*, 223-235.

[17] Bozner P, Wilson GL, Druzhyna NM, Bryant-Thomas TK, LeDoux SP, Pappolla MA (2002) Deficiency of chaperonin 60 in Down's syndrome. *J Alzheimers Dis* **4**, 479-486.
[18] Ogawa O, Perry G, Smith MA (2002) The "Down's" side of mitochondria. *Dev Cell* **2**, 255-256.
[19] Coskun PE, Wyrembak J, Derbereva O, Melkonian G, Doran E, Lott IT, Head E, Cotman CW, Wallace DC (2010) Systemic mitochondrial dysfunction and the etiology of Alzheimer's disease and down syndrome dementia. *J Alzheimers Dis* **20 Suppl 2**, S293-310.
[20] Valenti D, de Bari L, De Filippis B, Henrion-Caude A, Vacca RA (2014) Mitochondrial dysfunction as a central actor in intellectual disability-related diseases: An overview of Down syndrome, autism, Fragile X and Rett syndrome. *Neurosci Biobehav Rev*.
[21] Swomley AM, Forster S, Keeney JT, Triplett J, Zhang Z, Sultana R, Butterfield DA (2014) Abeta, oxidative stress in Alzheimer disease: evidence based on proteomics studies. *Biochim Biophys Acta* **1842**, 1248-1257.
[22] Reddy PH, Tripathi R, Troung Q, Tirumala K, Reddy TP, Anekonda V, Shirendeb UP, Calkins MJ, Reddy AP, Mao P, Manczak M (2012) Abnormal mitochondrial dynamics and synaptic degeneration as early events in Alzheimer's disease: implications to mitochondria-targeted antioxidant therapeutics. *Biochim Biophys Acta* **1822**, 639-649.
[23] Pelloquin F, Lamelin JP, Lenoir GM (1986) Human B lymphocytes immortalization by Epstein-Barr virus in the presence of cyclosporin A. *In Vitro Cell Dev Biol* **22**, 689-694.
[24] Campos PB, Sartore RC, Abdalla SN, Rehen SK (2009) Chromosomal spread preparation of human embryonic stem cells for karyotyping. *J Vis Exp*.
[25] Jaewon Lee SES, Douglas C. Wallace (2009) Adenine Nucleotide Translocator 1 Deficiency Increases Resistance of Mouse Brain and Neurons to Excitotoxic Insults by Inhibiting the Mitochondrial Permeability Transition Pore *Biochimica et Biophysica Acta, Bioenergetics*.
[26] Baracca A, Sgarbi G, Solaini G, Lenaz G (2003) Rhodamine 123 as a probe of mitochondrial membrane potential: evaluation of proton flux through F(0) during ATP synthesis. *Biochim Biophys Acta* **1606**, 137-146.
[27] Cocheme HM, Murphy MP (2008) Complex I is the major site of mitochondrial superoxide production by paraquat. *J Biol Chem* **283**, 1786-1798.
[28] Lee J, Schriner SE, Wallace DC (2009) Adenine nucleotide translocator 1 deficiency increases resistance of mouse brain and neurons to excitotoxic insults. *Biochim Biophys Acta* **1787**, 364-370.
[29] Moreno-Sanchez R, Rodriguez-Enriquez S, Marin-Hernandez A, Saavedra E (2007) Energy metabolism in tumor cells. *FEBS J* **274**, 1393-1418.
[30] Lee J, Giordano S, Zhang J (2012) Autophagy, mitochondria and oxidative stress: cross-talk and redox signalling. *Biochem J* **441**, 523-540.
[31] Shanware NP, Bray K, Abraham RT (2013) The PI3K, metabolic, and autophagy networks: interactive partners in cellular health and disease. *Annu Rev Pharmacol Toxicol* **53**, 89-106.
[32] Rossignol R, Gilkerson R, Aggeler R, Yamagata K, Remington SJ, Capaldi RA (2004) Energy substrate modulates mitochondrial structure and oxidative capacity in cancer cells. *Cancer Res* **64**, 985-993.
[33] de las Cuevas N, Urcelay E, Hermida OG, Saiz-Diaz RA, Bermejo F, Ayuso MS, Martin-Requero A (2003) Ca2+/calmodulin-dependent modulation of cell cycle elements pRb

and p27kip1 involved in the enhanced proliferation of lymphoblasts from patients with Alzheimer dementia. *Neurobiol Dis* **13**, 254-263.

[34] Wallace DC (2011) Bioenergetic origins of complexity and disease. *Cold Spring Harb Symp Quant Biol* **76**, 1-16.

[35] Murphy MP (2009) How mitochondria produce reactive oxygen species. *Biochem J* **417**, 1-13.

[36] Trounce IA, Kim YL, Jun AS, Wallace DC (1996) Assessment of mitochondrial oxidative phosphorylation in patient muscle biopsies, lymphoblasts, and transmitochondrial cell lines. *Methods Enzymol* **264**, 484-509.

[37] Perluigi M, Swomley AM, Butterfield DA (2014) Redox proteomics and the dynamic molecular landscape of the aging brain. *Ageing Res Rev* **13**, 75-89.

[38] Russell RC, Yuan HX, Guan KL (2014) Autophagy regulation by nutrient signaling. *Cell Res* **24**, 42-57.

[39] Kabeya Y, Mizushima N, Ueno T, Yamamoto A, Kirisako T, Noda T, Kominami E, Ohsumi Y, Yoshimori T (2000) LC3, a mammalian homologue of yeast Apg8p, is localized in autophagosome membranes after processing. *EMBO J* **19**, 5720-5728.

[40] Mizushima N, Yoshimori T (2007) How to interpret LC3 immunoblotting. *Autophagy* **3**, 542-545.

[41] Barth S, Glick D, Macleod KF (2010) Autophagy: assays and artifacts. *J Pathol* **221**, 117-124.

[42] Lee SH, Lee S, Jun HS, Jeong HJ, Cha WT, Cho YS, Kim JH, Ku SY, Cha KY (2003) Expression of the mitochondrial ATPase6 gene and Tfam in Down syndrome. *Mol Cells* **15**, 181-185.

[43] Piccoli C, Izzo A, Scrima R, Bonfiglio F, Manco R, Negri R, Quarato G, Cela O, Ripoli M, Prisco M, Gentile F, Cali G, Pinton P, Conti A, Nitsch L, Capitanio N (2013) Chronic pro-oxidative state and mitochondrial dysfunctions are more pronounced in fibroblasts from Down syndrome foeti with congenital heart defects. *Hum Mol Genet* **22**, 1218-1232.

[44] Aburawi EH, Souid AK (2012) Lymphocyte respiration in children with Trisomy 21. *BMC Pediatr* **12**, 193.

[45] Contestabile A, Fila T, Ceccarelli C, Bonasoni P, Bonapace L, Santini D, Bartesaghi R, Ciani E (2007) Cell cycle alteration and decreased cell proliferation in the hippocampal dentate gyrus and in the neocortical germinal matrix of fetuses with Down syndrome and in Ts65Dn mice. *Hippocampus* **17**, 665-678.

[46] Rueda N, Mostany R, Pazos A, Florez J, Martinez-Cue C (2005) Cell proliferation is reduced in the dentate gyrus of aged but not young Ts65Dn mice, a model of Down syndrome. *Neurosci Lett* **380**, 197-201.

[47] Williams BR, Prabhu VR, Hunter KE, Glazier CM, Whittaker CA, Housman DE, Amon A (2008) Aneuploidy affects proliferation and spontaneous immortalization in mammalian cells. *Science* **322**, 703-709.

[48] Capone G, Kim P, Jovanovich S, Payne L, Freund L, Welch K, Miller E, Trush M (2002) Evidence for increased mitochondrial superoxide production in Down syndrome. *Life Sci* **70**, 2885-2895.

[49] Du H, Guo L, Fang F, Chen D, Sosunov AA, McKhann GM, Yan Y, Wang C, Zhang H, Molkentin JD, Gunn-Moore FJ, Vonsattel JP, Arancio O, Chen JX, Yan SD (2008) Cyclophilin D deficiency attenuates mitochondrial and neuronal perturbation and ameliorates learning and memory in Alzheimer's disease. *Nat Med* **14**, 1097-1105.

[50] Gandhi S, Wood-Kaczmar A, Yao Z, Plun-Favreau H, Deas E, Klupsch K, Downward J, Latchman DS, Tabrizi SJ, Wood NW, Duchen MR, Abramov AY (2009) PINK1-associated Parkinson's disease is caused by neuronal vulnerability to calcium-induced cell death. *Mol Cell* **33**, 627-638.

[51] Rimessi A, Giorgi C, Pinton P, Rizzuto R (2008) The versatility of mitochondrial calcium signals: from stimulation of cell metabolism to induction of cell death. *Biochim Biophys Acta* **1777**, 808-816.

[52] Santo-Domingo J, Demaurex N (2010) Calcium uptake mechanisms of mitochondria. *Biochim Biophys Acta* **1797**, 907-912.

[53] Supnet C, Bezprozvanny I (2010) Neuronal calcium signaling, mitochondrial dysfunction, and Alzheimer's disease. *J Alzheimers Dis* **20 Suppl 2**, S487-498.

[54] Schuchmann S, Muller W, Heinemann U (1998) Altered Ca2+ signaling and mitochondrial deficiencies in hippocampal neurons of trisomy 16 mice: a model of Down's syndrome. *J Neurosci* **18**, 7216-7231.

[55] Chouhan AK, Ivannikov MV, Lu Z, Sugimori M, Llinas RR, Macleod GT (2012) Cytosolic calcium coordinates mitochondrial energy metabolism with presynaptic activity. *J Neurosci* **32**, 1233-1243.

[56] Canellada A, Ramirez BG, Minami T, Redondo JM, Cano E (2008) Calcium/calcineurin signaling in primary cortical astrocyte cultures: Rcan1-4 and cyclooxygenase-2 as NFAT target genes. *Glia* **56**, 709-722.

[57] Fernandez-Martinez P, Zahonero C, Sanchez-Gomez P (2015) DYRK1A: the double-edged kinase as a protagonist in cell growth and tumorigenesis. *Mol Cell Oncol* **2**, e970048.

[58] Peiris H, Duffield MD, Fadista J, Jessup CF, Kashmir V, Genders AJ, McGee SL, Martin AM, Saiedi M, Morton N, Carter R, Cousin MA, Kokotos AC, Oskolkov N, Volkov P, Hough TA, Fisher EM, Tybulewicz VL, Busciglio J, Coskun PE, Becker A, Belichenko PV, Mobley WC, Ryan MT, Chan JY, Laybutt DR, Coates PT, Yang S, Ling C, Groop L, Pritchard MA, Keating DJ (2016) A Syntenic Cross Species Aneuploidy Genetic Screen Links RCAN1 Expression to beta-Cell Mitochondrial Dysfunction in Type 2 Diabetes. *PLoS Genet* **12**, e1006033.

[59] Lepagnol-Bestel AM, Zvara A, Maussion G, Quignon F, Ngimbous B, Ramoz N, Imbeaud S, Loe-Mie Y, Benihoud K, Agier N, Salin PA, Cardona A, Khung-Savatovsky S, Kallunki P, Delabar JM, Puskas LG, Delacroix H, Aggerbeck L, Delezoide AL, Delattre O, Gorwood P, Moalic JM, Simonneau M (2009) DYRK1A interacts with the REST/NRSF-SWI/SNF chromatin remodelling complex to deregulate gene clusters involved in the neuronal phenotypic traits of Down syndrome. *Hum Mol Genet* **18**, 1405-1414.

[60] Gottlieb E, Armour SM, Harris MH, Thompson CB (2003) Mitochondrial membrane potential regulates matrix configuration and cytochrome c release during apoptosis. *Cell Death Differ* **10**, 709-717.

[61] Attar A, Ripoli C, Riccardi E, Maiti P, Li Puma DD, Liu T, Hayes J, Jones MR, Lichti-Kaiser K, Yang F, Gale GD, Tseng CH, Tan M, Xie CW, Straudinger JL, Klarner FG, Schrader T, Frautschy SA, Grassi C, Bitan G (2012) Protection of primary neurons and mouse brain from Alzheimer's pathology by molecular tweezers. *Brain* **135**, 3735-3748.

[62] Carmeliet G, David G, Cassiman JJ (1991) Cellular ageing of Alzheimer's disease and Down syndrome cells in culture. *Mutat Res* **256**, 221-231.

[63] Di Domenico F, Barone E, Perluigi M, Butterfield DA (2014) Strategy to reduce free radical species in Alzheimer's disease: an update of selected antioxidants. *Expert Rev Neurother*, 1-22.
[64] Zigman WB (2013) Atypical aging in Down syndrome. *Dev Disabil Res Rev* **18**, 51-67.
[65] Mao P, Reddy PH (2011) Aging and amyloid beta-induced oxidative DNA damage and mitochondrial dysfunction in Alzheimer's disease: implications for early intervention and therapeutics. *Biochim Biophys Acta* **1812**, 1359-1370.
[66] Black AT, Gray JP, Shakarjian MP, Laskin DL, Heck DE, Laskin JD (2008) Increased oxidative stress and antioxidant expression in mouse keratinocytes following exposure to paraquat. *Toxicol Appl Pharmacol* **231**, 384-392.
[67] Ermak G, Davies KJ (2013) Chronic high levels of the RCAN1-1 protein may promote neurodegeneration and Alzheimer disease. *Free Radic Biol Med* **62**, 47-51.
[68] Shaw JL, Chang KT (2013) Nebula/DSCR1 upregulation delays neurodegeneration and protects against APP-induced axonal transport defects by restoring calcineurin and GSK-3beta signaling. *PLoS Genet* **9**, e1003792.
[69] Soppa U, Schumacher J, Florencio Ortiz V, Pasqualon T, Tejedor FJ, Becker W (2014) The Down syndrome-related protein kinase DYRK1A phosphorylates p27(Kip1) and Cyclin D1 and induces cell cycle exit and neuronal differentiation. *Cell Cycle* **13**, 2084-2100.
[70] Boya P, Reggiori F, Codogno P (2013) Emerging regulation and functions of autophagy. *Nat Cell Biol* **15**, 713-720.
[71] Scherz-Shouval R, Elazar Z (2011) Regulation of autophagy by ROS: physiology and pathology. *Trends Biochem Sci* **36**, 30-38.

Table 1: Age distribution of the samples. All the samples were selected as Caucasian to reduce the ethic variability. From each sex, we used 4 to 6 samples for each assay. (AD; Alzheimer Disease, DS; Down syndrome, DSAD; Down Syndrome with dementia)

	Control		AD		DS		DSAD	
Sex	ID	Age	ID	Age	ID	Age	ID	Age
male	CM1	41	AM1	55	DM1	41	DAM1	45
	CM2	44	AM2	57	DM2	47	DAM1	47
	CM3	52	AM3	57	DM3	51	DAM3	48
	CM4	57	AM4	60	DM4	51	DAM1	48
	CM5	61	AM5	60	DM5	53	DAM1	49
	CM6	62	AM6	60	DM6	54	DAM3	51
	CM7	63	AM7	62	DM7	55	DAM1	51
			AM8	68	DM8	55	DAM1	52
					DM9	56	DAM3	56
					DM10	57	DAM1	58
					DM11	60	DAM1	58
					DM12	60	DAM3	60
							DAM1	64
							DAM1	69
Female	CF1	49	AF1	55	DF1	42	DAF1	40
	CF2	50	AF2	60	DF2	48	DAF2	40
	CF3	53	AF3	66	DF3	51	DAF3	42
	CF4	54	AF4	67	DF4	51	DAF4	53
	CF5	56	AF5	70	DF5	52	DAF5	57
	CF6	66	AF6	75	DF6	57	DAF6	57
	CF7	68			DF7	57		
					DF8	59		
					DF9	59		
					DF10	59		
					DF11	60		

Table 2: Summary chart of the changes observed in DS, DSAD and AD compared to Control LCLs levels.

	DS	DSAD	AD
Mitochondrial Membrane Potential	↓	↓	↓
Mitochondrial calcium sequestration	=	↓	↓
Cellular Growth under glucose[#]	↓	↓	=
Cellular Growth under galactose[#]	↓↓	↓	=
Change of ATP levels under RAO	=	↓	↓
Basal cellular ROS levels	↑↑	=	=
pQ induced ROS levels*	↑	↑↑	↑
mROS levels under oxidative metabolism	↑	=	↑
mROS levels under glycolytic metabolism	↓	↓	↓
LC3-II levels at glycolysis	↓	↓	↓
LC3-II levels at oxidative metabolism	↓	=	=

*: compared to their individual baseline ROS levels, [#]:minimal feeding
↓:reduced *($p<0.05$),* ↑:increased *($p<0.05$)*, ↓:increased *($p=0.06$),* =No Change.
RAO: **R**otenone, **A**ntimycin, **O**ligomycin (mitochondrial inhibitors); mROS: **m**itochondrial **R**eactive **O**xygen **S**pecies; pQ: **p**ara**Q**uat(oxidative toxin); LC3-II: Autophagy marker.

Figure Legends

Figure 1. Reduced mitochondrial membrane potential and differential calcium uptake in DS, DSAD and AD LCLs. A. Mitochondrial membrane potential (ΔΨ) expressed in millivolts (mV) was quantified in LCLs from AD, DS and DSAD lines, and compared to age-matched controls. DS, DSAD and AD LCLs exhibit lower ΔΨ (*p=0.03, ANOVA).* **B**. Quantification of total calcium required to induce mitochondrial permeability pore opening. AD and DSAD LCLs exhibited significantly lower buffering capacity *(p<0.05)* while there was no difference between DS and control LCLs.

Figure 2. Impaired proliferative capacity in DS and DSAD LCLs. Cellular proliferation of LCLs in glucose- (**A**) and galactose-containing medium (**B**) was assessed during 15 days. **A:** Both DS and DSAD LCLs exhibited slow proliferation in glucose. The difference was evident starting at day 5 *(p=0.001 ANOVA).* All four groups reached the growth plateau around day 12. However, the final number of cells in DS and DSAD LCLs (~$6x10^6$cells/10ml) was markedly lower compared to control LCLs (~$1.2x\ 10^7$cells/10ml). **B:** All four groups exhibited slower proliferation rates in galactose than in glucose. DS LCLs showed modest proliferation at all time points while DSAD LCLs significantly slowed down proliferation after day 7. Thus, marked differences were observed between DS and DSAD at day 7 and thereafter *(p=0.039 ANOVA).*

Figure 3. Cellular and mitochondrial oxidative stress in LCLs. A. Cellular ROS were quantified using the fluorescent probe DCFDA. Baseline (BL) levels are indicated by a white bar. Paraquat (pQ) was added to the culture medium to increase cellular ROS production (shown as red bar). Black and red dotted lines indicate control ROS levels at baseline and after pQ administration respectively. DS LCLs exhibited significantly higher cellular ROS at baseline *(p=0.04, ANOVA)*. DSAD LCLs showed significantly higher ROS production after pQ treatment *(p<0.05, two way ANOVA; individual p values are indicated on the panel)*. **B.** Baseline mitochondrial oxidative stress measured with the fluorescent probe mitoSOX in glucose- and galactose-containing medium. Ratio of galactose primed LCL to glucose primed LCL (white bars) levels as well as the antimycin treated galactose primed LCLs to glucose primed LCLs in individual groups was measured. Although control galactose-primed cells showed similar levels

of oxidative stress than in glucose medium (ratio~1), DS, DSAD and AD groups showed increased oxidative stress under galactose conditions (*p=0.035 two way ANOVA;* media effect). Additionally, 30 minute antimycin treatment in galactose primed LCLs showed more ROS than expected in all groups though the difference did not reach significance. **C.** Total ATP levels in LCLs at baseline and after 30 min of treatment with RAO in glucose medium. The results are presented as the percentage change in ATP level after RAO treatment compared to baseline. The red dashed line represents the individual group's baseline. DSAD and AD lines exhibited a significant reduction in ATP levels after RAO treatment *(*p<0.05 ANOVA)*. DS lines also showed a trend of reduction in ATP levels *(p>0.05 ANOVA)*. (RFU: Relative fluorescent unit)

Figure 4. Differential LC3-II expression levels in DS, DSAD and AD LCLs. Protein levels of LC3-II represented in glucose primed (**A**) and galactose primed (**B**) control, DS, DSAD and AD LCLs. LC3-II levels were reduced in glucose-primed DS, DSAD and AD LCLs compared to controls (**A,** ***p<0.006, *p=0.03, •p=0.06 ANOVA, respectively)*. However, only DS LCLs showed a significant reduction of LC3-II under galactose-primed medium (**B,** *p<0.003, ANOVA)*. In addition, LC3-II levels were significantly lower in all four groups of LCLs primed with galactose compared to the same groups maintained in glucose-containing medium (*two way AcNOVA p<0.001*, note that y-axes scales of graph A and B are different, RFU: Relative fkeurassr).

Supporting Information Legend

Figure S1. Similar growth rate in DS, DSAD, AD and control LCLs under standard feeding conditions. A. Glucose and **B.** Galactose primed LCLs were analyzed for 15 days. All four groups of LCLs demonstrated similar growth pattern. LCL proliferation was significantly slower under galactose supplementation compared to glucose for all four groups of LCLs (Note that the y-axes scales are different between the graphs).

Figure 1. Reduced mitochondrial membrane potential and differential calcium uptake in DS, DSAD and AD LCLs.

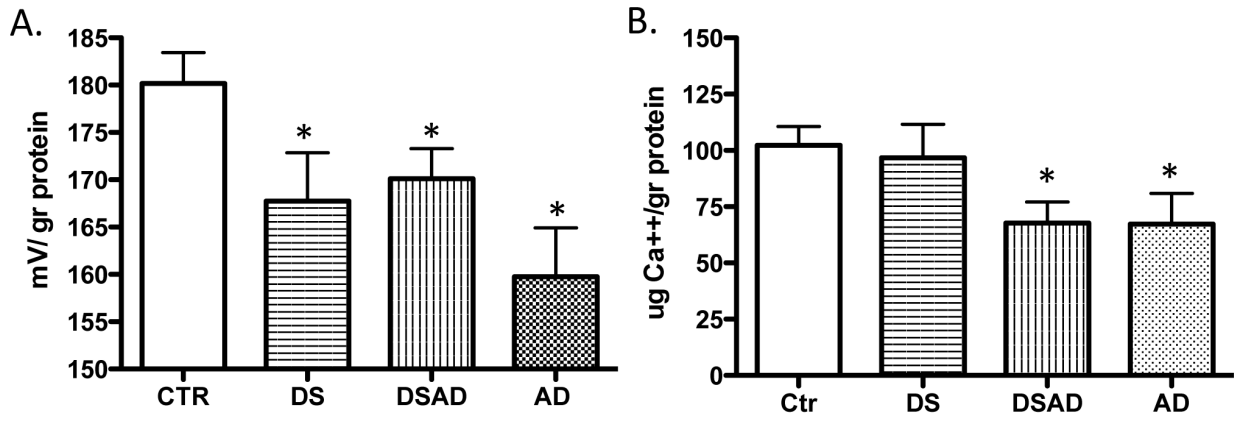

Figure 2. Impaired proliferative capacity in DS and DSAD LCLs.

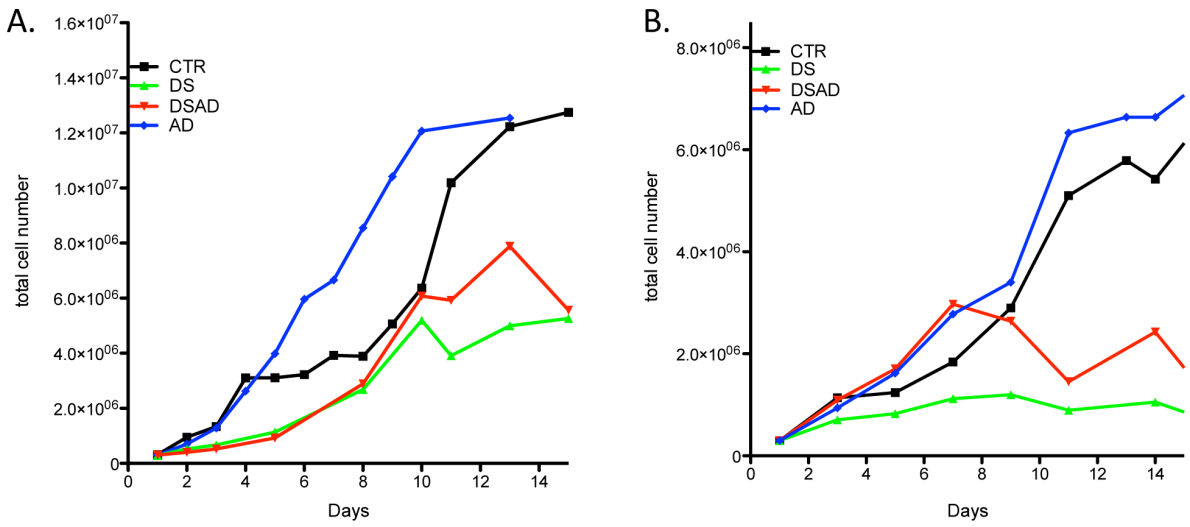

Figure 3. Cellular and mitochondrial oxidative stress in LCLs.

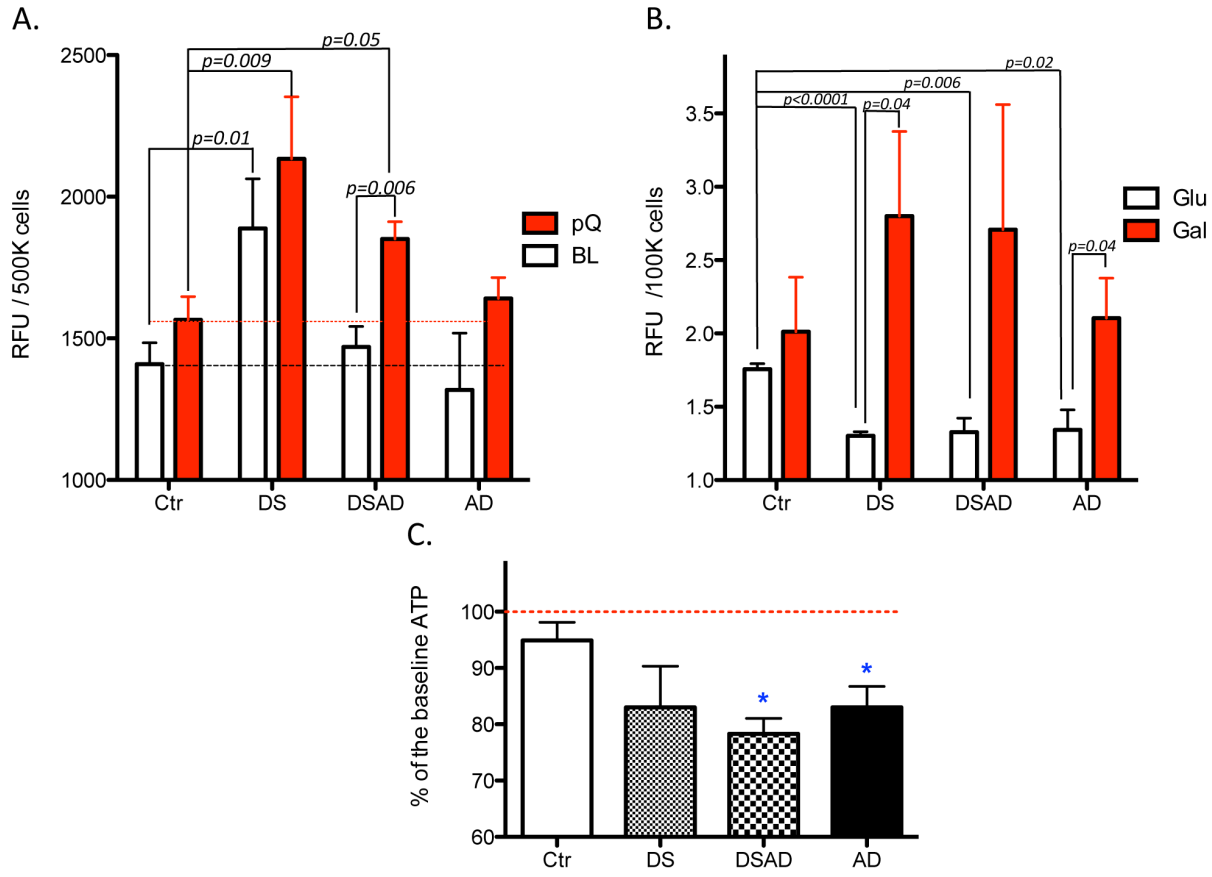

Figure 4. Differential LC3-II expression levels in DS, DSAD and AD LCLs.

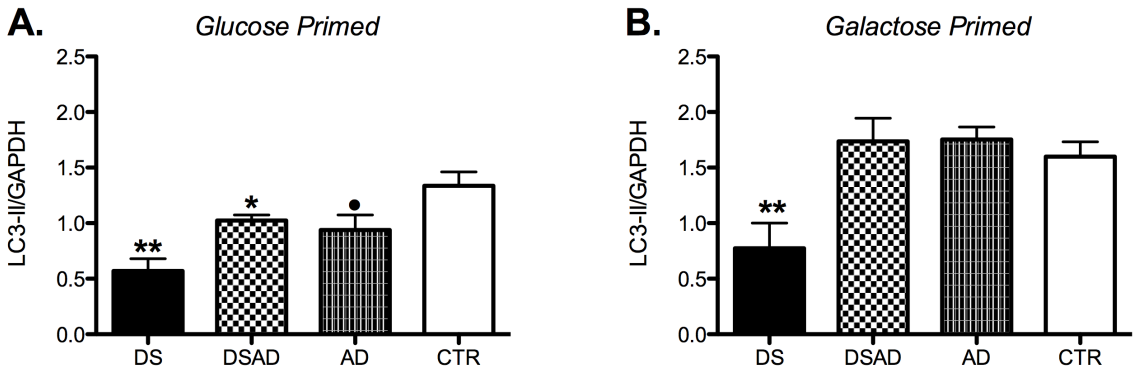

Figure S1. Similar growth rate in DS, DSAD, AD and control LCLs under standard feeding conditions.